
Hi-VAE: Efficient Video Autoencoding with Global and Detailed Motion

Huaize Liu^{1,3*†}, Wenzhang Sun^{2*}, Qiyuan Zhang⁴, Donglin Di², Biao Gong⁵, Hao Li²,
Chen Wei², Changqing Zou^{3,4‡},

¹University of Chinese Academy of Sciences, ²Li Auto, ³Zhejiang Lab,
⁴State Key Lab of CAD&CG, Zhejiang University, ⁵Ant Group

Abstract

Recent breakthroughs in video autoencoders (Video AEs) have advanced video generation, but existing methods fail to efficiently model spatio-temporal redundancies in dynamics, resulting in suboptimal compression factors. This shortfall leads to excessive training costs for downstream tasks. To address this, we introduce Hi-VAE, an efficient video autoencoding framework that hierarchically encode coarse-to-fine motion representations of video dynamics and formulate the decoding process as a conditional generation task. Specifically, Hi-VAE decomposes video dynamics into two latent spaces: Global Motion, capturing overarching motion patterns, and Detailed Motion, encoding high-frequency spatial details. Using separate self-supervised motion encoders, we compress video latents into compact motion representations to reduce redundancy significantly. A conditional diffusion decoder then reconstructs videos by combining hierarchical global and detailed motions, enabling high-fidelity video reconstructions. Extensive experiments demonstrate that Hi-VAE achieves a high compression factor of $1428\times$, almost $30\times$ higher than baseline methods (e.g., Cosmos-VAE at $48\times$), validating the efficiency of our approach. Meanwhile, Hi-VAE maintains high reconstruction quality at such high compression rates and performs effectively in downstream generative tasks. Moreover, Hi-VAE exhibits interpretability and scalability, providing new perspectives for future exploration in video latent representation and generation.

1 Introduction

The latent diffusion model (LDM) has revolutionized image generation via its core image autoencoder, which encodes images into a compact latent space to reduce modeling complexity and enhance training efficiency. Adapting this framework to video is challenging due to spatio-temporal dynamics: video latent spaces must encode both visual content and temporal consistency, posing unique design challenges for effective encoders.

Previous video autoencoders [33, 23, 1, 52, 22, 43, 38, 41] typically encode individual frames or frame groups into fixed-dimensional latent vectors. For example, Cosmos-VAE [1] achieves a compression factor of $48\times$ by downsampling videos with spatial factor 8 and temporal factor 4. However, such methods fail to model spatiotemporal redundancy inherent in videos, leaving significant room for improved compression efficiency (Fig. 1 (a)). In video sequences, global motion patterns exhibit repetitive dynamics. Therefore, coarse video dynamics can be compressed across both spatial and temporal dimensions to achieve higher compression ratios. Subsequently, fine-grained frame details

*Equal Contribution.

†Work done as interns at Li Auto.

‡Corresponding author.

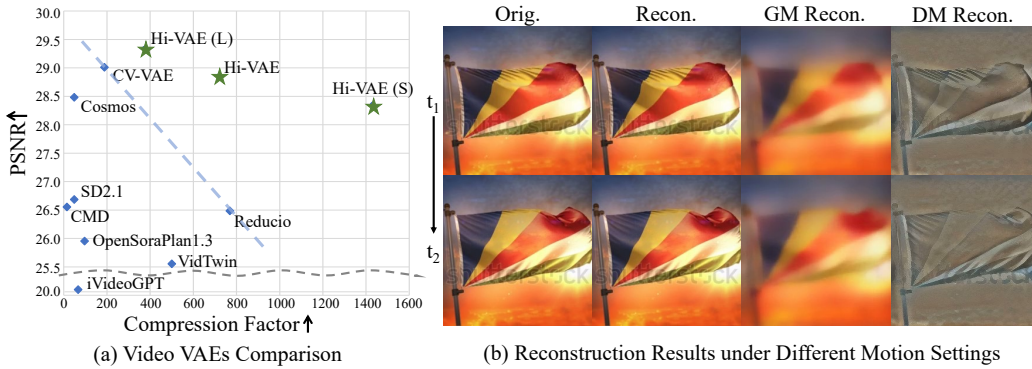


Figure 1: (a) **Video VAEs comparison.** State-of-the-art Video VAEs are evaluated on WebVid-10M validation dataset at 256×256 resolution. Performance is measured using PSNR, which is balanced against the compression factor, defined as the ratio between the size of the input video and the latent space. Our Hi-VAE, designed with three different sizes of motion latents, outperforms the respective baselines, achieving state-of-the-art results. (b) **Example reconstructions.** For frames t_1 and t_2 , we display the original video frames (Orig.), reconstructed frames (Recon.), frames reconstructed using only Global Motion (GM Recon.) and using only Detailed Motion (DM Recon.). Global Motion captures the primary semantic content and global motion patterns, while Detailed Motion captures high-frequency details and fast movements.

can be further compacted through spatial dimension encoding (Fig. 1 (b)). By comprehensively exploiting spatiotemporal redundancies, we can derive an efficient and compact latent representation.

In this paper, we propose **Hi-VAE**, an efficient **Video AutoEncoder** designed for **H**ierarchically encoding video dynamics. Hi-VAE employs a two-stage coarse-to-fine encoding process, initially compressing spatiotemporal dynamics into compact representations to reconstruct a coarse video and subsequently refining it with detailed spatial motion information. Hi-VAE decomposes video dynamics into two latent spaces: **Global Motion**, capturing overarching motion patterns, and **Detailed Motion**, encoding high-frequency spatial details. Based on this compact motion representation, we introduce a diffusion-based decoder that integrates latent motions to enable high-fidelity video generation (Fig. 1). To the best of our knowledge, Hi-VAE is the first diffusion-based video autoencoder.

Specifically, Hi-VAE models video dynamics via a Hierarchical Motion Encoder and reconstructs through a Conditional Diffusion Decoder. Motion latents are self-supervised learned with distinct objectives: (1) *Global Motion Extraction Module* employs low-pass filtering and cross-attention with learnable queries to focus on relevant spatio-temporal motion; (2) *Detailed Motion Extraction Module* uses high-pass filtering and per-frame tokens via self-attention for fine-grained details; (3) *Conditional Diffusion Decoder*, built on flow-matching, integrates motion components to perform coarse-to-fine refinement: encoding global motion for coarse dynamics and incorporating detailed motion to refine spatial details. To enhance motion representation learning, a two-stage training strategy is proposed: the model first pretrains global motion extraction followed by end-to-end fine-tuning to integrate detailed motion, boosting overall performance.

Through experiments on the WebVid-10M [2] dataset, Hi-VAE outperforms baseline methods with superior reconstruction quality and a higher compression factor (up to $1400\times$), demonstrating its efficiency (Fig. 1 (a)). Additionally, experiments on the UCF-101 [36] dataset confirm the effectiveness of downstream task, achieving performance comparable to well-established models. Moreover, through extensive experiments, we demonstrate that the extracted motion latents exhibit both interpretability and scalability, thereby providing avenues for future research and improvement. The main contributions can be summarized as follows:

- Building on the motivation of coarse-to-fine compression and reconstruction, we propose a efficient diffusion-based video autoencoder, Hi-VAE. This innovative architecture provides a new perspective for efficient video encoding and decoding.
- We hierarchically extract global and detailed motion to compress spatio-temporal redundancy while preserving details. Meanwhile, our Conditional Diffusion Decoder ensures high-fidelity video reconstruction even under extreme compression.

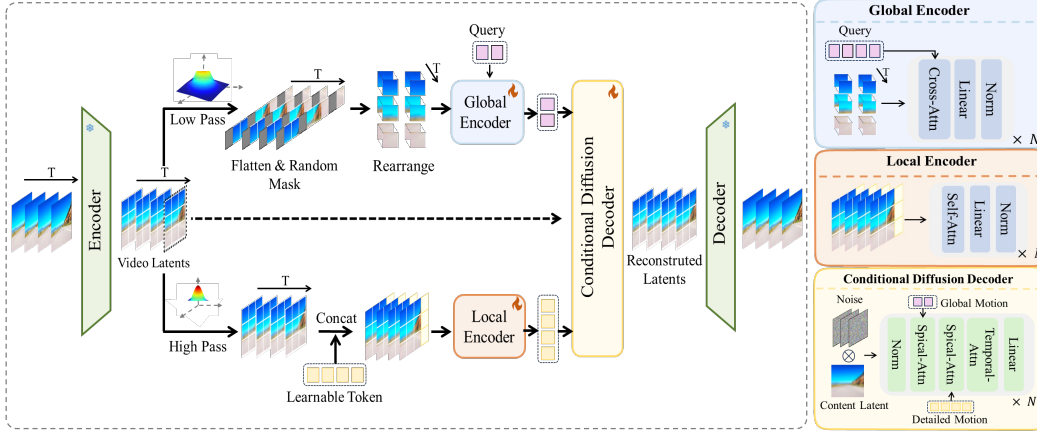


Figure 2: **Architecture of Hi-VAE.** After obtaining the latent variable z from the encoder, we leverage the Global Motion Module and Detailed Motion Module to extract hierarchical motion features. Subsequently, the Conditional Diffusion Decoder fuses the motion latents with the content latent to generate the predicted \hat{z} , which is then decoded into the reconstructed video frames. The internal structure of each key module is also illustrated.

- Extensive experiments demonstrate our method’s efficiency via high compression rates and superior reconstruction quality. We further validate its low training overhead and effectiveness in generative tasks, while confirming the interpretability and scalability of the extracted motion latents.

2 Related Work

2.1 Visual Compression

Recent advances in visual generation have spurred significant interest in visual compression and latent representation learning [34, 11, 47, 13, 49, 17, 5, 32]. Leading methods typically compress visual content from pixel space into a lower-dimensional latent space, as exemplified by the 2D VAE used in Stable Diffusion [33]. For video data, 3D convolutions [3, 35, 23, 53, 1, 28] and spatio-temporal attention [15, 18, 42, 45, 12, 27, 54, 40] have been employed to capture temporal dynamics. Cosmos [1] adopts a lightweight, temporally causal architecture enabling unified and order-preserving tokenization across images and videos of arbitrary length. Due to redundancy between adjacent frames, direct video compression is often inefficient. To improve this, some methods disentangle content and motion, enabling more compact representations [34, 11, 38, 48, 41, 49]. Reducio-VAE [38] introduces a factorized, image-conditioned 3D VAE that compresses video into motion latent guided by a single content frame. CMD [48] approximates content using a weighted average of frames, while motion is learned separately. VidTwin [41] disentangles video into structure and dynamics latent vectors for independent modeling of spatial and temporal factors. Despite the ability of these methods to achieve smaller compression ratios, they may introduce distortions or result in the loss of high-frequency details. In this work, we revisit the decoupling paradigm and propose a new formulation that addresses these limitations. Our experiments demonstrate its strong potential, offering a promising direction for future research.

2.2 Diffusion Autoencoders

Diffusion models have demonstrated strong performance in visual generation tasks [7, 33, 8, 25, 44, 37, 30, 10], with simplified variants such as Rectified Flow improving efficiency and sample quality [26, 24]. Leveraging this, Diffusion Autoencoders [31] first proposed using a diffusion decoder for end-to-end autoencoding, inspiring a line of work exploring diffusion autoencoders for representation learning and perceptual image compression [19, 4, 46]. Recent efforts extend this framework with discrete latent variables: ϵ -VAE [51] introduces a GAN-based tokenizer trained with perceptual and adversarial losses. While these efforts have primarily focused on image compression, diffusion-based decoding remains underexplored in the context of video. In this work, we extend diffusion autoencoding to the video domain by introducing a tailored DIT-based decoder. Our approach improves not only the reconstruction fidelity of fine-grained visual details but also enhances temporal consistency and motion realism in reconstructed video sequences.

3 Method

A standard Variational Autoencoder (VAE) encodes video inputs into a compressed latent space. Given a video $x \in \mathbb{R}^{C \times F \times H \times W}$, where C, F, H, W represent the channel, number of frames, height, and width respectively, the encoder \mathcal{E} maps x to a latent representation $z = \mathcal{E}(x) \in \mathbb{R}^{c \times f \times h \times w}$ with reduced spatiotemporal resolution. The decoder \mathcal{D} reconstructs the input as $\hat{x} = \mathcal{D}(z) = \mathcal{D}(\mathcal{E}(x))$, ensuring end-to-end learning of a compressed latent distribution.

In our Hi-VAE model, we extract hierarchical motion representations from videos and reconstruct the videos by leveraging motion and content latent. As illustrated in Fig. 2, after obtaining the latent vector z , we use two compression modules, Enc_ϕ^G and Enc_ψ^D , to obtain the global motion u_g and detailed motion u_d . Enc_ϕ^G denotes the Global Motion Extraction Module with parameters ϕ , while Enc_ψ^D denotes the Detailed Motion Extraction Module with parameters ψ . The encoding procedures are described in Sec. 3.1. For decoding, we employ a flow-matching based DIT model, Dec_θ , to integrate diverse motion and content latents c from first frame feature, and finally reconstruct the video, which are described in Sec. 3.2. The overall procedure is summarized as follows:

$$u_g, u_d = Enc_\phi^G(\mathcal{E}(x)), Enc_\psi^D(\mathcal{E}(x)) \quad (1)$$

$$\hat{x} = \mathcal{D}(Dec_\theta(u_g; u_d; c)) \quad (2)$$

In Sec. 3.3, we outline the training and inference pipelines, and lastly, in Sec. 3.4, we discuss a design for adapting our proposed latent for use with generation models.

3.1 Encode Compressed Representation from Video

As shown in Fig. 2, the latent vector z is processed by the Global Motion Extraction Module and the Detailed Motion Extraction Module to obtain the global motion u_g and detailed motion u_d .

3.1.1 Extracting Global Motion

To extract global motion patterns from video dynamics, the latent vector z is first passed through a frequency filter to obtain the low-frequency representation z_{low} . The process can be described as:

$$z_{\text{low}} = \text{IFFT}_{3\text{D}}(\text{FFT}_{3\text{D}}(z) \odot \mathcal{P}) \quad (3)$$

where $\text{FFT}_{3\text{D}}$ and $\text{IFFT}_{3\text{D}}$ denote the 3D Fast Fourier Transform and its inverse, applied across spatial and temporal dimensions to project to and from the frequency domain. $\mathcal{P} \in \mathbb{R}^{c \times f \times h \times w}$ is the spatial-temporal Low Pass Filter (LPF), which is a tensor of the same shape as the latent z . To extract coarse temporal dynamics, a Global Encoder is then employed. To focus on temporal variation while minimizing spatial influence, we spatially flatten the input and apply a spatial mask M , with masking ratios uniformly sampled between 30% and 50%. Higher masking ratios promote abstraction by filtering out spatial detail. The result latent is rearranged by folding spatial dimensions into the batch, yielding $z_g \in \mathbb{R}^{(hw) \times f \times c}$. Then we introduce a learnable query $q_g \in \mathbb{R}^{f_g \times n_g \times c_g}$, where f_g is half the number of frames, n_g is the token number and c_g is the channel dimension, enabling spacial-temporal compression. A Transformer architecture is used to extract global motion features from the video dynamics. In each block, the motion latent z_g serves as the key and value, while the learnable token q_g acts as the query in a cross-attention mechanism. The final global motion representation u_g is obtained as:

$$z_g = \text{Rearrange}(\text{Flatten}(z_{\text{low}}) \odot M), \quad (4)$$

$$u_g = \text{softmax}(q_g z_g^T / \sqrt{d}) z_g \quad (5)$$

3.1.2 Incorporating Detailed Motion

While the global motion branch captures coarse dynamics, it overlooks high-frequency details and rapid local movements. To address this, we extract fine-grained motion by focusing on spatial variations. This approach allows us to preserve critical high-frequency components that are otherwise lost in global motion representations. Initially, the latent vector z is passed through a high-pass filter to obtain high-frequency latent z_{high} . The process can be described as:

$$z_{\text{high}} = \text{IFFT}_{3\text{D}}(\text{FFT}_{3\text{D}}(z) \odot (1 - \mathcal{P})) \quad (6)$$

Subsequently, we introduce a learnable detailed motion token $q_d \in \mathbb{R}^{f_d \times n_d \times c_d}$, where f_d is the number of frames, n_d is the token number and c_d is the channel dimension. The tokens are concatenated with the high-frequency latent representation z_{high} along the temporal dimension. To facilitate effective extraction of fine-grained, high-frequency motion information, we perform self-attention over the concatenated frame-wise latent. The process can be described as:

$$z_d = z_{\text{high}} \otimes q_d, \quad (7)$$

$$u_d = \text{softmax}(z_d z_d^T / \sqrt{d}) z_d \quad (8)$$

Finally, we extract the learnable token component from u_d as the final detailed motion representation.

3.2 Decode Video from Compressed Representation

After obtaining the Global Motion and Detailed Motion, our objective is to reconstruct high-fidelity videos by leveraging both coarse-grained and fine-grained motion information. To enrich appearance and structure, the first frame is embedded as the content latent c . To achieve high-quality video reconstruction and to better integrate different motion representations, we adopt a flow-matching-based Conditional Diffusion Decoder built on the DiT architecture [29]. Specifically, we first add noise to the video latent vector z , then the repeated content latent c is concatenated with the noised video latent, as the decoder input z_t . To inject motion control into the decoding process, the global motion u_g and detailed motion u_d are also concatenated with z_t respectively, followed by self-attention to enable effective integration of motion cues. To ensure temporal coherence, a Temporal Align Block (TAB) merges the time axis into the batch dimension, enabling temporal modeling via self-attention. $\{z_t^f\}_{f=1}^k = \text{TAB}(\{z_t^f\}_{f=1}^k)$, where k is the number of frames. The overall process is described as:

$$z_t = ((1-t)z + t\epsilon) \otimes c, \quad (9)$$

$$\hat{v} = \text{Dec}_\theta(z_t, u_g, u_d, t) \quad (10)$$

where ϵ denotes Gaussian Noise sampled from standard normal distribution, $t \in [0, 1]$ denotes the noise intensity and \hat{v} denotes the predicted noise velocity. Then the ODE solver takes the estimated velocity \hat{v} to compute the latent vector \hat{z} , which is subsequently used to reconstruct the final video \hat{x} .

3.3 Training and Inference

Following a coarse-to-fine strategy, we adopt a two-stage training strategy. In the first stage, the Hi-VAE is trained using only the Global Motion Extraction Module on blurred video data. In the second stage, the parameters of the Global Motion Extraction Module are frozen, and the Hi-VAE is further trained with the addition of the Detailed Motion Extraction Module on high-fidelity video data. The decoder predicts noise velocity, optimized via the mean squared error between the predicted velocity \hat{v} and ground-truth velocity $v = z - \epsilon$. To further regularize the distribution of motion latents for compatibility with the generative model, we incorporate a KL divergence loss with the standard Gaussian distribution $\mathcal{L}_{KL} = KL(\mathcal{N}(\mu_v, \sigma_v) || \mathcal{N}(\mathbf{0}, \mathbf{I}))$. The final loss is defined as:

$$\min_{\phi, \delta} \mathcal{L}_{\text{first stage}} = \mathbb{E}_{t, z_t, z, \epsilon} \left[\left\| (z - \epsilon) - v_\delta(z_t, \text{Enc}_\phi^G(z), t) \right\|^2 \right] + \lambda_{KL} \mathcal{L}_{KL} \quad (11)$$

$$\min_{\psi, \gamma} \mathcal{L}_{\text{second stage}} = \mathbb{E}_{t, z_t, z, \epsilon} \left[\left\| (z - \epsilon) - v_\gamma(z_t, \text{Enc}_\phi^G(z), \text{Enc}_\psi^D(z), t) \right\|^2 \right] + \lambda_{KL} \mathcal{L}_{KL} \quad (12)$$

where v_δ and v_γ denotes the predicted velocity. During inference, the input video is encoded to extract the global motion u_g and detailed motion u_d . We then sample the generating vector field from noise ϵ and predict the noise velocity \hat{v} using u_g, u_d and content latent c . Finally, the ODE solver takes the estimated velocity to compute the latent vector \hat{z} via numerical integration.

3.4 Conditional Video Generation with Hi-VAE

To validate the superiority of Hi-VAE in downstream generative tasks, we design a flow-matching-based motion generation model. Specifically, we first use the pre-trained Hi-VAE to extract Global Motion $u_g \in \mathbb{R}^{f_g \times n_g \times c_g}$ and Detailed Motion $u_d \in \mathbb{R}^{f_d \times n_d \times c_d}$. Both are projected into a unified channel dimension c_m using a multi-layer perceptron (MLP). We then normalize them to a comparable scale and concatenate them along the token length dimension to obtain the final training target motion $m \in \mathbb{R}^{f \times (n_g + n_d) \times c_m}$. Our generative model is a standard DiT [29] model. Following the rectified



Figure 3: **Qualitative comparison with baseline methods.** We showcase three examples: a scene with slow transformations, a rapidly changing boxing scene, and a local facial transformation. Hi-VAE exhibits superior reconstruction performance across diverse motion types.

flow [26], noise ϵ is added to the m , and the model is trained to predict the noise velocity \hat{v} . The loss function optimizes the mean squared distance between the \hat{v} and the true velocity $m - \epsilon$. During the sampling, we generate the motion latent \hat{m} with classifier-free guidance, then decode it using Hi-VAE to produce the final video. For additional implementation details on the diffusion process, please refer to the corresponding section in the Appendix A.3.

4 Experiment

4.1 Experiment setup

Dataset. We train and evaluate our model mainly on the WebVid-10M dataset [2] with 10 million video-text pairs. Considering its diverse content and motion speeds, this dataset is ideal for design realization and model validation. To assess the generative capacity and adaptability of the model’s latent representations, we conduct class-conditioned video generation on UCF-101 [36], which provides 101 different classes of motion videos.

Implementation Details. We train and evaluate our model on 256×256 video clips at 8 fps, with each clip containing 16 frames. We split videos with higher resolutions into tiles in the spatial dimension. Unless otherwise specified, all results are based on a unified latent representation with Global Motion $u_g \in \mathbb{R}^{8 \times 8 \times 8}$ and Detailed Motion $u_d \in \mathbb{R}^{16 \times 16 \times 16}$. More details about regarding the model architecture and training resource overhead are provided in the Appendix A.

Evaluation Metrics and Baseline. We evaluate the reconstruction performance of Hi-VAE using standard reconstruction metrics, including PSNR [18], SSIM [42], LPIPS [50], reconstruction FID (rFID) [14] and reconstruction FVD (rFVD) [39]. Additionally, we report the Compression Rate (Comp. Rate), defined as the ratio between the the dimension of the latent space used in the downstream generative model and the original input video. To ensure comprehensive comparison, we benchmark against state-of-the-art baselines across two categories: (1) **content VAE**

Table 1: **Quantitative Comparison.** Red indicates the best result, blue the second-best, and green the third-best. For various Hi-VAE configurations, "S" represents small and "L" represents large. In the user study, "Deta." denotes detail quality, "Sema." denotes semantic preservation, and "Temp." denotes temporal consistency. Our model outperforms baselines across these metrics.

Methods		Comp. Rate	PSNR \uparrow	SSIM \uparrow	LPIPS \downarrow	rFID \downarrow	rFVD \downarrow	Deta. \uparrow	Semo. \uparrow	Temp. \uparrow
content VAE	SD2.1-VAE [6]	2.08%	26.684	0.813	0.106	5.591	81.785	4.68	4.36	4.47
	OpenSoraPlan1.3-VAE [23]	1.04%	25.953	0.792	0.110	6.157	78.883	4.64	4.52	4.52
	Cosmos-VAE [1]	2.08%	28.481	0.830	0.105	6.449	121.986	4.73	4.74	4.83
	CV-VAE [52]	0.53%	29.008	0.825	0.099	4.030	86.162	4.76	4.71	4.77
content-motion VAE	iVideoGPT [43]	1.50%	20.713	0.5594	0.326	18.677	356.904	3.71	3.88	3.92
	CMD [48]	6.85%	26.553	0.795	0.110	11.664	98.623	4.65	4.41	4.58
	Reducio [38]	0.13%	26.484	0.786	0.112	7.334	108.936	4.46	4.54	4.69
	VidTwin [41]	0.20%	25.530	0.799	0.119	11.941	131.059	4.32	4.26	4.48
	Hi-VAE (S)	0.07%	28.365	0.808	0.109	5.425	74.005	4.71	4.76	4.82
	Hi-VAE	0.14%	28.861	0.826	0.101	5.227	71.278	4.81	4.78	4.85
	Hi-VAE (L)	0.27%	29.347	0.834	0.096	4.002	61.941	4.85	4.82	4.88

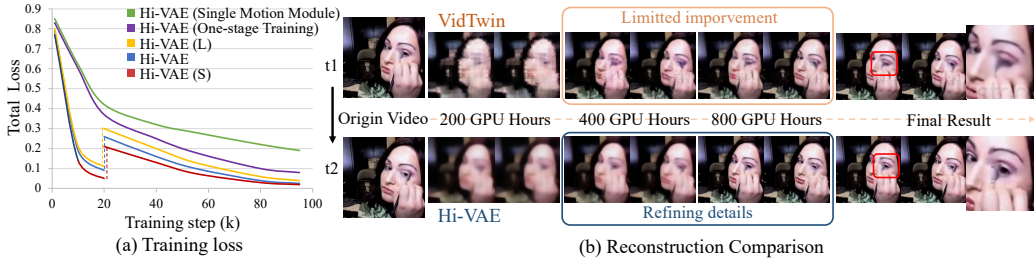


Figure 4: Fig. (a) **Training loss** under different settings is shown. Fig. (b) **Reconstruction results** of Hi-VAE and VidTwin during training steps and after training completion are presented.

encodes individual frames as fixed-dimensional latent vectors, including SD2.1-VAE [33], Open-Sora-Plan1.3-VAE [23], Cosmos-VAE [1], and CV-VAE [52]; and (2) **content-motion VAE** decomposes representations into static content (via reference frames) and dynamic motion (via frame transitions), enabling video generation by synthesizing only the motion latent, such as iVideoGPT [43], Reducio [38], CMD [48], and VidTwin [41]. This setup allows us to assess the benefits of our proposed design in both reconstruction fidelity and compression ratio. We also conducted a user study involving 20 expert evaluators. Each participant rated 20 video samples based on three perceptual criteria: detail quality, semantic preservation, and temporal consistency. Ratings were assigned on a 5-point Likert scale, and the final score for each method was reported as the Mean Opinion Score (MOS), averaged across all raters and categories. More details refer to Appendix C.1.

4.2 Reconstruction Quality

As shown in Tab. 1, our method outperforms baselines on most objective and subjective metrics, achieving high reconstruction quality with a lower compression rate. Notably, most content-motion VAEs achieve lower compression rates than content VAEs by disentangling motion and content representations. However, these methods typically sacrifice spatial detail and semantic fidelity, resulting in lower reconstruction performance. Encouragingly, our method—despite being a content-motion VAE—achieves both lower compression and competitive or better reconstruction quality than content VAE baselines. Results from the user study further confirm that our model outperforms baselines in perceived detail, semantic preservation, and temporal consistency.

As illustrated in Fig. 3, we further conducted qualitative evaluations across three representative motion types: (1) slow and smooth, (2) rapid and dynamic, and (3) fine-grained localized motion. For slow motion (left), most baseline methods—except VidTwin and iVideoGPT—achieved stable reconstructions. Under rapid motion (middle), baselines suffered semantic and structural degradation, with CV-VAE retaining global structure but showing detail distortions. In fine-grained cases (right), baselines exhibited detail loss and facial deformation. Notably, VidTwin trained on WebVid-10M introduced watermark-like artifacts, suggesting dataset overfitting. Our method consistently preserved both semantic integrity and fine-level details across all cases, demonstrating robust performance under diverse motion conditions. Comprehensive qualitative experiments with content VAEs and content-motion VAEs are provided in the Appendix B.1.

Table 2: **Generative ability** of our model and the baselines on UCF-101.

Methods	FID ↓	FVD ↓
Video-LaViT [20]	25.822	204.661
iVideoGPT [43]	28.304	254.881
CMD [48]	22.304	198.332
Hi-VAE	24.809	210.881

Table 3: **Ablation studies** on the proposed techniques

Methods	PSNR↑	SSIM↑	rFID ↓
w/o hierarchical.	23.831	0.724	9.665
w/o freq.	26.322	0.752	7.965
w/o diffusion dec.	24.304	0.701	10.838
w/o two-stage train.	27.603	0.791	6.827
Hi-VAE	28.861	0.826	5.227

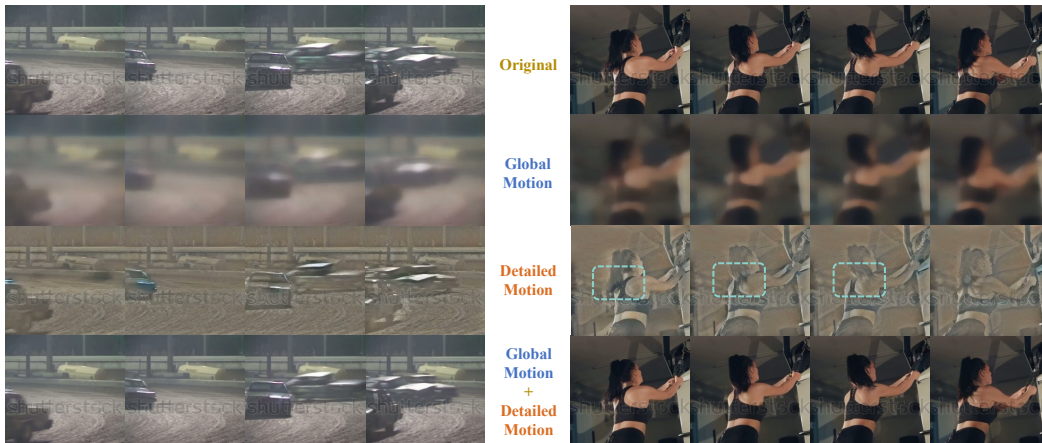


Figure 5: **Reconstruction results under different motions**, including the original video, the reconstructed outputs, and outputs using only Global Motion or Detailed Motion.

To evaluate scalability, we train our architecture under varying motion latent configurations: small ($u_g \in \mathbb{R}^{8 \times 8 \times 4}$, $u_d \in \mathbb{R}^{16 \times 16 \times 8}$), normal ($u_g \in \mathbb{R}^{8 \times 8 \times 8}$, $u_d \in \mathbb{R}^{16 \times 16 \times 16}$) and large ($u_g \in \mathbb{R}^{8 \times 8 \times 8}$, $u_d \in \mathbb{R}^{16 \times 16 \times 32}$). As shown in Tab. 1, reconstruction quality improves with larger motion latents, which we attribute to the design of our transformer-based encoder and flow-matching-based decoder. We also conducted qualitative experiments under different motion latent configurations, details can be found in Appendix B.2. To validate the generalizability of our model, we supplemented the reconstruction results on additional datasets, including RealEstate-10K [55] and UCF-101 [36]. Moreover, we incorporated further reconstruction results derived from the WebVid-10M dataset. These results demonstrate the generalizability and superior reconstruction capabilities of our approach, as detailed in Appendix D.

4.3 Further Analysis

Training Efficiency. Our hierarchical motion modules enable the model to learn distinct semantic spaces, leading to more efficient reconstruction training. To further promote disentanglement and accelerate convergence, we adopt a two-stage training strategy, which improves both training stability and speed. As shown in Fig. 4 (a), our method achieves faster loss convergence compared to single-module or one-stage training baselines, highlighting its optimization efficiency. Notably, lower-dimensional motion latents slow convergence due to increased semantic compactness. Fig. 4 (b) compares reconstruction performance with VidTwin under the same training steps, showing that Hi-VAE enables more efficient training and achieves higher reconstruction quality both during the training process and after convergence.

Explorations on the Roles of Latents. As described in Sec. 3.2, our decoder employs separate modules to integrate global motion and detailed motion. This design allows independent analysis of each motion stream by generating outputs conditioned on either global motion or detailed motion alone. As illustrated in Fig. 5, global motion captures coarse dynamics (e.g., overall vehicle movement, body contours) and produces blurrier, low-frequency reconstructions, while detailed motion models fine-grained variations (e.g., fast deformations, flickering hair) requiring larger latent size to retain high-frequency motion. This distinction highlights the interpretability and complementary nature of the hierarchical motion representation.

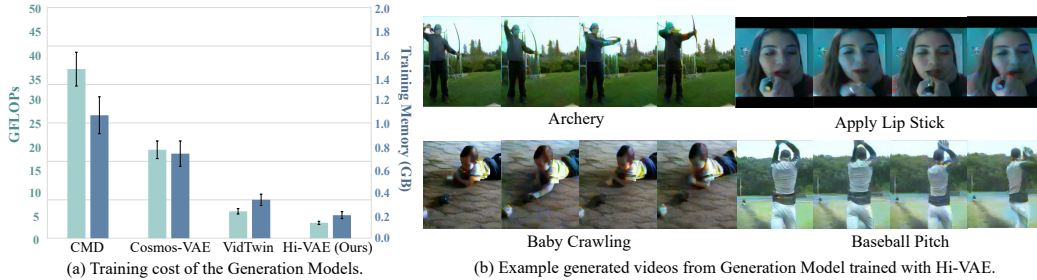


Figure 6: Fig. (a) presents the FLOPs and training memory costs of the unified generative model of our model and the baselines. The values were measured after averaging over 10 dataset splits and an error bar means standard deviation. Fig. (b) showcases the video generation results on the UCF-101 dataset using the generative model designed based on Hi-VAE.

Analysis for Generative Models. Our video autoencoder generates highly compressed hierarchical motion latents, which significantly reduces the computational cost of downstream generative tasks and thereby enhances the efficiency of generative models. To validate this, we compare the FLOPs and memory consumption of generative models against representative baselines. We construct a standardized DiT architecture [29] to ensure fair comparisons focused solely on resource usage rather than generation quality. As shown in Fig. 6 (a), models operating on Hi-VAE’s compact latents require significantly fewer FLOPs and less memory. The low-dimensional design also supports smaller diffusion backbones, further enhancing deployment efficiency. More details regarding the standardized DiT are provided in Appendix C.2

As demonstrated in Sec. 3.4, we further implement a lightweight DiT-based generative framework conditioned on Hi-VAE latents and evaluate it on the UCF-101 dataset for class-conditional video generation. Tab. 2 and Fig. 6 (b) report quantitative and qualitative results, respectively. While not aiming for SOTA, our approach shows good visual quality and temporal consistency, verifying the latent space’s compatibility with diffusion models. We expect enhanced generative performance with improved designs, larger datasets, and advanced training techniques. Additional details about generation model are provided in the Appendix A.3

4.4 Ablation Studies

We conducted an ablation study to evaluate the actual impact of our proposed designs. All experiments were performed under the same number of training steps, and the results are summarized in Tab. 3. The key findings are as follows: (1) Replacing hierarchical motion modules (hierarchical.) with a single module causes significant performance degradation and as in Fig. 4 (a), lower training efficiency. In contrast, our Hierarchical Motion Compression captures both high and low frequencies, improving reconstruction quality and training efficiency. (2) When the frequency filter (freq.) is removed, the model performance degrades. This is because the filter helps the two motion modules to focus separately on coarse-grained and fine-grained semantics, thereby enabling better reconstruction results. (3) Replacing the diffusion decoder (diffusion dec.) with a transformer block trained purely with reconstruction loss leads to a significant performance decline. This suggests that the flow-based decoder is more effective in learning distinct motion semantics and achieving superior reconstruction guided by motion latents. (4) Employing a one-stage training strategy instead of a two-stage training strategy (two-stage train.) weakens the model’s ability to learn coarse-grained and fine-grained motions separately, resulting in a degradation of the reconstruction result quality. As shown in Fig 4 (a), this approach also reduces training efficiency.

5 Conclusion and Limitations

Video generation holds immense potential, yet remains constrained by prohibitive computational costs. In this work, we introduced Hi-VAE, an efficient hierarchical video autoencoding framework. Our encoder decomposes spatio-temporal dynamics into global and detailed motion using specialized extraction modules in a hierarchical manner. To reconstruct high-fidelity video, we propose a flow-matching-based conditional diffusion decoder that integrates hierarchical motion and content latents. Extensive experiments demonstrate that our method is effective, achieving an exceptionally low compression rate of 0.07% and state-of-the-art reconstruction quality. Building on Hi-VAE, we

design a lightweight video generation model that achieves competitive performance in both resource efficiency and generation quality, demonstrating strong adaptability to downstream tasks.

Limitations and future work. We find that lower-dimensional motion latents slow convergence and degrade details in reconstruction. Additionally, Our lightweight generation model mainly validates Hi-VAE’s adaptability. Designing more efficient and principled generation models remains an open direction. Moreover, the semantic hierarchical motion representations from Hi-VAE show potential for video understanding and camera-controlled generation, which we aim to explore further.

References

- [1] Niket Agarwal, Arslan Ali, Maciej Bala, Yogesh Balaji, Erik Barker, Tiffany Cai, Prithvijit Chattopadhyay, Yongxin Chen, Yin Cui, Yifan Ding, et al. Cosmos world foundation model platform for physical ai. *arXiv preprint arXiv:2501.03575*, 2025.
- [2] Max Bain, Arsha Nagrani, Gül Varol, and Andrew Zisserman. Frozen in time: A joint video and image encoder for end-to-end retrieval. In *Proceedings of the IEEE/CVF international conference on computer vision*, pages 1728–1738, 2021.
- [3] Omer Bar-Tal, Hila Chefer, Omer Tov, Charles Herrmann, Roni Paiss, Shiran Zada, Ariel Ephrat, Junhwa Hur, Guanghui Liu, Amit Raj, et al. Lumiere: A space-time diffusion model for video generation. In *SIGGRAPH Asia 2024 Conference Papers*, pages 1–11, 2024.
- [4] Vighnesh Birodkar, Gabriel Barcik, James Lyon, Sergey Ioffe, David Minnen, and Joshua V Dillion. Sample what you cant compress. *arXiv preprint arXiv:2409.02529*, 2024.
- [5] Andreas Blattmann, Tim Dockhorn, Sumith Kulal, Daniel Mendelevitch, Maciej Kilian, Dominik Lorenz, Yam Levi, Zion English, Vikram Voleti, Adam Letts, et al. Stable video diffusion: Scaling latent video diffusion models to large datasets. *arXiv preprint arXiv:2311.15127*, 2023.
- [6] Andreas Blattmann, Robin Rombach, Huan Ling, Tim Dockhorn, Seung Wook Kim, Sanja Fidler, and Karsten Kreis. Align your latents: High-resolution video synthesis with latent diffusion models. In *Proceedings of the IEEE/CVF conference on computer vision and pattern recognition*, pages 22563–22575, 2023.
- [7] Tim Brooks, Bill Peebles, Connor Holmes, Will DePue, Yufei Guo, Li Jing, David Schnurr, Joe Taylor, Troy Luhman, Eric Luhman, et al. Video generation models as world simulators. *OpenAI Blog*, 1:8, 2024.
- [8] Haoxin Chen, Yong Zhang, Xiaodong Cun, Menghan Xia, Xintao Wang, Chao Weng, and Ying Shan. Videocrafter2: Overcoming data limitations for high-quality video diffusion models. In *Proceedings of the IEEE/CVF Conference on Computer Vision and Pattern Recognition*, pages 7310–7320, 2024.
- [9] Kingma Diederik. Adam: A method for stochastic optimization. (*No Title*), 2014.
- [10] Patrick Esser, Sumith Kulal, Andreas Blattmann, Rahim Entezari, Jonas Müller, Harry Saini, Yam Levi, Dominik Lorenz, Axel Sauer, Frederic Boesel, et al. Scaling rectified flow transformers for high-resolution image synthesis. In *Forty-first international conference on machine learning*, 2024.
- [11] Yue Gao, Jiahao Li, Lei Chu, and Yan Lu. Implicit motion function. In *Proceedings of the IEEE/CVF Conference on Computer Vision and Pattern Recognition*, pages 19278–19289, 2024.
- [12] Yuwei Guo, Ceyuan Yang, Anyi Rao, Zhengyang Liang, Yaohui Wang, Yu Qiao, Maneesh Agrawala, Dahua Lin, and Bo Dai. Animatediff: Animate your personalized text-to-image diffusion models without specific tuning. *arXiv preprint arXiv:2307.04725*, 2023.
- [13] Tianyu He, Junliang Guo, Runyi Yu, Yuchi Wang, Jialiang Zhu, Kaikai An, Leyi Li, Xu Tan, Chunyu Wang, Han Hu, et al. Gaia: Zero-shot talking avatar generation. *arXiv preprint arXiv:2311.15230*, 2023.

- [14] Martin Heusel, Hubert Ramsauer, Thomas Unterthiner, Bernhard Nessler, and Sepp Hochreiter. Gans trained by a two time-scale update rule converge to a local nash equilibrium. *Advances in neural information processing systems*, 30, 2017.
- [15] Jonathan Ho, Ajay Jain, and Pieter Abbeel. Denoising diffusion probabilistic models. *Advances in neural information processing systems*, 33:6840–6851, 2020.
- [16] Jonathan Ho and Tim Salimans. Classifier-free diffusion guidance. *arXiv preprint arXiv:2207.12598*, 2022.
- [17] Wenyi Hong, Ming Ding, Wendi Zheng, Xinghan Liu, and Jie Tang. Cogvideo: Large-scale pretraining for text-to-video generation via transformers. *arXiv preprint arXiv:2205.15868*, 2022.
- [18] Alain Hore and Djemel Ziou. Image quality metrics: Psnr vs. ssim. In *2010 20th international conference on pattern recognition*, pages 2366–2369. IEEE, 2010.
- [19] Drew A Hudson, Daniel Zoran, Mateusz Malinowski, Andrew K Lampinen, Andrew Jaegle, James L McClelland, Loic Matthey, Felix Hill, and Alexander Lerchner. Soda: Bottleneck diffusion models for representation learning. In *Proceedings of the IEEE/CVF Conference on Computer Vision and Pattern Recognition*, pages 23115–23127, 2024.
- [20] Yang Jin, Zhicheng Sun, Kun Xu, Liwei Chen, Hao Jiang, Quzhe Huang, Chengru Song, Yuliang Liu, Di Zhang, Yang Song, et al. Video-lavit: Unified video-language pre-training with decoupled visual-motional tokenization. *arXiv preprint arXiv:2402.03161*, 2024.
- [21] Diederik P Kingma, Max Welling, et al. Auto-encoding variational bayes, 2013.
- [22] Weijie Kong, Qi Tian, Zijian Zhang, Rox Min, Zuozhuo Dai, Jin Zhou, Jiangfeng Xiong, Xin Li, Bo Wu, Jianwei Zhang, et al. Hunyuanvideo: A systematic framework for large video generative models. *arXiv preprint arXiv:2412.03603*, 2024.
- [23] Bin Lin, Yunyang Ge, Xinhua Cheng, Zongjian Li, Bin Zhu, Shaodong Wang, Xianyi He, Yang Ye, Shenghai Yuan, Liuhan Chen, et al. Open-sora plan: Open-source large video generation model. *arXiv preprint arXiv:2412.00131*, 2024.
- [24] Yaron Lipman, Ricky TQ Chen, Heli Ben-Hamu, Maximilian Nickel, and Matt Le. Flow matching for generative modeling. *arXiv preprint arXiv:2210.02747*, 2022.
- [25] Huaize Liu, Wenzhang Sun, Donglin Di, Shibo Sun, Jiahui Yang, Changqing Zou, and Hujun Bao. Moe: Mixture of emotion experts for audio-driven portrait animation. *arXiv preprint arXiv:2501.01808*, 2025.
- [26] Xingchao Liu, Chengyue Gong, and Qiang Liu. Flow straight and fast: Learning to generate and transfer data with rectified flow. *arXiv preprint arXiv:2209.03003*, 2022.
- [27] Xin Ma, Yaohui Wang, Gengyun Jia, Xinyuan Chen, Ziwei Liu, Yuan-Fang Li, Cunjian Chen, and Yu Qiao. Latte: Latent diffusion transformer for video generation. *arXiv preprint arXiv:2401.03048*, 2024.
- [28] Mizuho Nishio, Chihiro Nagashima, Saori Hirabayashi, Akinori Ohnishi, Kaori Sasaki, Tomoyuki Sagawa, Masayuki Hamada, and Tatsuo Yamashita. Convolutional auto-encoder for image denoising of ultra-low-dose ct. *Heliyon*, 3(8), 2017.
- [29] William Peebles and Saining Xie. Scalable diffusion models with transformers. In *Proceedings of the IEEE/CVF international conference on computer vision*, pages 4195–4205, 2023.
- [30] Dustin Podell, Zion English, Kyle Lacey, Andreas Blattmann, Tim Dockhorn, Jonas Müller, Joe Penna, and Robin Rombach. Sdxl: Improving latent diffusion models for high-resolution image synthesis. *arXiv preprint arXiv:2307.01952*, 2023.
- [31] Konpat Preechakul, Nattanat Chatthee, Suttisak Wizadwongsa, and Supasorn Suwajanakorn. Diffusion autoencoders: Toward a meaningful and decodable representation. In *Proceedings of the IEEE/CVF conference on computer vision and pattern recognition*, pages 10619–10629, 2022.

- [32] Sucheng Ren, Qihang Yu, Ju He, Xiaohui Shen, Alan Yuille, and Liang-Chieh Chen. Flowar: Scale-wise autoregressive image generation meets flow matching. *arXiv preprint arXiv:2412.15205*, 2024.
- [33] Robin Rombach, Andreas Blattmann, Dominik Lorenz, Patrick Esser, and Björn Ommer. High-resolution image synthesis with latent diffusion models. In *Proceedings of the IEEE/CVF conference on computer vision and pattern recognition*, pages 10684–10695, 2022.
- [34] Aliaksandr Siarohin, Stéphane Lathuilière, Sergey Tulyakov, Elisa Ricci, and Nicu Sebe. First order motion model for image animation. *Advances in neural information processing systems*, 32, 2019.
- [35] Uriel Singer, Adam Polyak, Thomas Hayes, Xi Yin, Jie An, Songyang Zhang, Qiyuan Hu, Harry Yang, Oron Ashual, Oran Gafni, et al. Make-a-video: Text-to-video generation without text-video data. *arXiv preprint arXiv:2209.14792*, 2022.
- [36] Khurram Soomro, Amir Roshan Zamir, and Mubarak Shah. Ucf101: A dataset of 101 human actions classes from videos in the wild. *arXiv preprint arXiv:1212.0402*, 2012.
- [37] Wenzhang Sun, Xiang Li, Donglin Di, Zhuding Liang, Qiyuan Zhang, Hao Li, Wei Chen, and Jianxun Cui. Uniavatar: Taming lifelike audio-driven talking head generation with comprehensive motion and lighting control. *arXiv preprint arXiv:2412.19860*, 2024.
- [38] Rui Tian, Qi Dai, Jianmin Bao, Kai Qiu, Yifan Yang, Chong Luo, Zuxuan Wu, and Yungang Jiang. Reducio! generating 1024times1024 video within 16 seconds using extremely compressed motion latents. *arXiv preprint arXiv:2411.13552*, 2024.
- [39] Thomas Unterthiner, Sjoerd Van Steenkiste, Karol Kurach, Raphael Marinier, Marcin Michalski, and Sylvain Gelly. Towards accurate generative models of video: A new metric & challenges. *arXiv preprint arXiv:1812.01717*, 2018.
- [40] Yaohui Wang, Xinyuan Chen, Xin Ma, Shangchen Zhou, Ziqi Huang, Yi Wang, Ceyuan Yang, Yinan He, Jiashuo Yu, Peiqing Yang, et al. Lavie: High-quality video generation with cascaded latent diffusion models. *International Journal of Computer Vision*, 133(5):3059–3078, 2025.
- [41] Yuchi Wang, Junliang Guo, Xinyi Xie, Tianyu He, Xu Sun, and Jiang Bian. Vidtwi: Video vae with decoupled structure and dynamics. *arXiv preprint arXiv:2412.17726*, 2024.
- [42] Zhou Wang, Alan C Bovik, Hamid R Sheikh, and Eero P Simoncelli. Image quality assessment: from error visibility to structural similarity. *IEEE transactions on image processing*, 13(4):600–612, 2004.
- [43] Jialong Wu, Shaofeng Yin, Ningya Feng, Xu He, Dong Li, Jianye Hao, and Mingsheng Long. ivideopt: Interactive videopts are scalable world models. *Advances in Neural Information Processing Systems*, 37:68082–68119, 2024.
- [44] Jiaqi Xu, Xinyi Zou, Kunzhe Huang, Yunkuo Chen, Bo Liu, MengLi Cheng, Xing Shi, and Jun Huang. Easyanimate: A high-performance long video generation method based on transformer architecture. *arXiv preprint arXiv:2405.18991*, 2024.
- [45] Wilson Yan, Yunzhi Zhang, P. Abbeel, and A. Srinivas. Videopt: Video generation using vq-vae and transformers. *ArXiv*, abs/2104.10157, 2021.
- [46] Ruihan Yang and Stephan Mandt. Lossy image compression with conditional diffusion models. *Advances in Neural Information Processing Systems*, 36:64971–64995, 2023.
- [47] Lijun Yu, Yong Cheng, Kihyuk Sohn, José Lezama, Han Zhang, Huiwen Chang, Alexander G Hauptmann, Ming-Hsuan Yang, Yuan Hao, Irfan Essa, et al. Magvit: Masked generative video transformer. In *Proceedings of the IEEE/CVF Conference on Computer Vision and Pattern Recognition*, pages 10459–10469, 2023.
- [48] Sihyun Yu, Weili Nie, De-An Huang, Boyi Li, Jinwoo Shin, and Anima Anandkumar. Efficient video diffusion models via content-frame motion-latent decomposition. *arXiv preprint arXiv:2403.14148*, 2024.

- [49] Qiyuan Zhang, Chenyu Wu, Wenzhang Sun, Huaize Liu, Donglin Di, Wei Chen, and Changqing Zou. Semantic latent motion for portrait video generation, 2025.
- [50] Richard Zhang, Phillip Isola, Alexei A Efros, Eli Shechtman, and Oliver Wang. The unreasonable effectiveness of deep features as a perceptual metric. In *Proceedings of the IEEE conference on computer vision and pattern recognition*, pages 586–595, 2018.
- [51] Long Zhao, Sanghyun Woo, Ziyu Wan, Yandong Li, Han Zhang, Boqing Gong, Hartwig Adam, Xuhui Jia, and Ting Liu. *epsilon*-vae: Denoising as visual decoding. *arXiv preprint arXiv:2410.04081*, 2024.
- [52] Sijie Zhao, Yong Zhang, Xiaodong Cun, Shaoshu Yang, Muyao Niu, Xiaoyu Li, Wenbo Hu, and Ying Shan. Cv-vae: A compatible video vae for latent generative video models. *arXiv preprint arXiv:2405.20279*, 2024.
- [53] Tingting Zhong, Xin Jin, and Kedeng Tong. 3d-cnn autoencoder for plenoptic image compression. In *2020 IEEE International Conference on Visual Communications and Image Processing (VCIP)*, pages 209–212. IEEE, 2020.
- [54] Daquan Zhou, Weimin Wang, Hanshu Yan, Weiwei Lv, Yizhe Zhu, and Jiashi Feng. Magicvideo: Efficient video generation with latent diffusion models. *arXiv preprint arXiv:2211.11018*, 2022.
- [55] Tinghui Zhou, Richard Tucker, John Flynn, Graham Fyffe, and Noah Snavely. Stereo magnification: Learning view synthesis using multiplane images. *arXiv preprint arXiv:1805.09817*, 2018.

A Implementation Details

A.1 Model Details

As described in Sec. 3.1, Hi-VAE adopts an Encoder-Decoder architecture. Specifically, we utilize transformer block in encoder and decoder. The Global Motion Extraction Module and Detailed Motion Extraction Module each consist of 8 transformer layers with 8 attention heads per layer. Both modules contain approximately 25 M parameters. The decoder consists of 16 layers and has a total of 640 M parameters. We experiment with motion latents of various dimensional configurations.

A.2 Training and Inference Details

The model is trained using $8 \times$ NVIDIA A800 GPUs, each with 80 GB of memory, and evaluated on an NVIDIA GeForce RTX 4090 GPU with 20 GB of memory. The model is trained the Adam optimizer with a learning rate of $1e-4$. The training process consists of two phases. In the first phase, the model is trained for 20,000 steps, amounting to approximately 200 GPU hours. In the second phase, the model undergoes an additional 80,000 steps of training, totaling approximately 750 GPU hours.

The decoder in our model is a Conditional Diffusion Decoder based on flow-matching. The diffusion process comprises 1000 steps for training and 20 steps for inference. We apply classifier-free guidance [16], randomly dropping conditioning in 10% of the samples during the training phase. The classifier-free guidance weight is set to 5 during the sampling process.

Table 4: Training Configuration

Parameter	Value
Input Video Resolution	256
Input Video Frames	16
Input Video FPS	8
Optimizer	Adam; $\beta_1 = 0.9, \beta_2 = 0.99$
Learning Rate	1×10^{-4}
Warmup Steps	5000
Learning Rate Scheduler	Cosine Annealing
\mathcal{L}_{KL}	0.001
Weight Decay	0.0001
Training Batch Size	8
Training Device	$8 \times 80G$ A800 GPUs

A.3 Video Generation Model Details

As detailed in Sec. 3.4, we present the design of a video generation diffusion model customized for the motion latents encoded by our Hi-VAE model. This model employs the DiT [29] architecture, consisting of 16 layers with a hidden state size of 1152. Each layer incorporates a cross-attention module to introduce conditionality and a temporal self-attention module to ensure temporal consistency of the generated motion sequences. For the UCF-101 dataset [36], we encode class information using a 128-dimensional vector. The generative model is grounded in Rectified flow [26], with the diffusion process spanning 1000 steps during training and 20 steps for inference. Classifier-free guidance is applied, randomly dropping conditionality in 20% of samples during training, and the classifier-free guidance weight is set to 5 during sampling.

For training, we adopt the Adam optimizer [21] with $\beta_1 = 0.9$ and $\beta_2 = 0.999$. The learning rate is regulated by a Lambda scheduler featuring 10,000 warmup steps. The training process is executed on

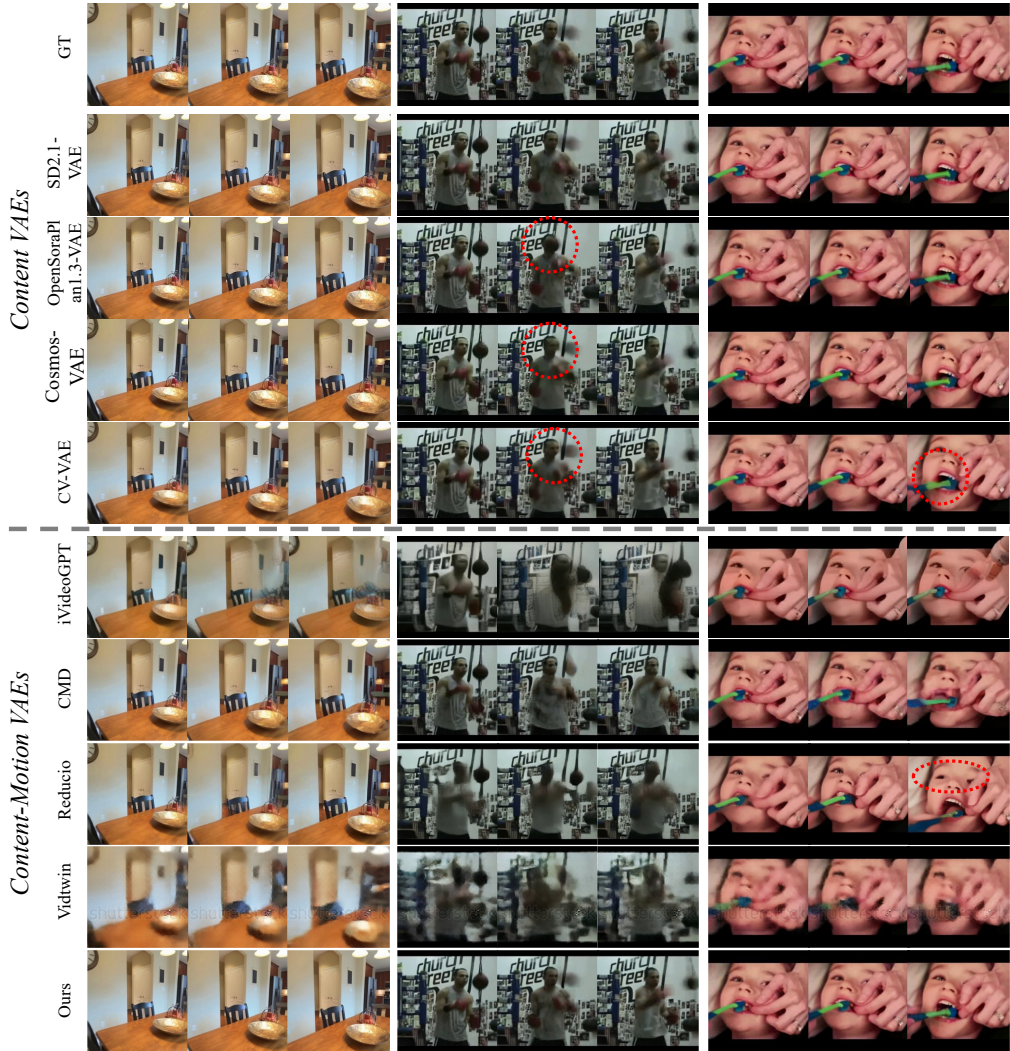


Figure 7: **Qualitative Comparison** with content VAE and content-motion VAE baselines.

8 × 80G A800 GPUs, with an input configuration of 16 video frames at a resolution of 256×256 and a frame rate of 16 fps.

B Additional Analysis for Hi-VAE

B.1 Comprehensive Qualitative Experiments

As shown in Fig. 7, we conducted comprehensive qualitative evaluations encompassing both content VAEs and content-motion VAEs. Three distinct motion categories were compared: (1) slow and smooth scene transitions, (2) rapid and dynamic boxing sequences, and (3) fine-grained facial expressions. Results indicate that while content VAEs generally outperform content-motion VAEs in reconstruction quality, they tend to lose fine details during high-frequency motion changes. In contrast, our method consistently preserves both semantic integrity and fine-grained details across all scenarios, demonstrating robust performance under diverse motion dynamics.

B.2 Qualitative Experiments under Different Configurations

We compare varying motion latent configurations: Hi-VAE (S), Hi-VAE and Hi-VAE (L). As shown in Fig. 8, we evaluate four distinct motion types: scene movement, object movement, fine-grained

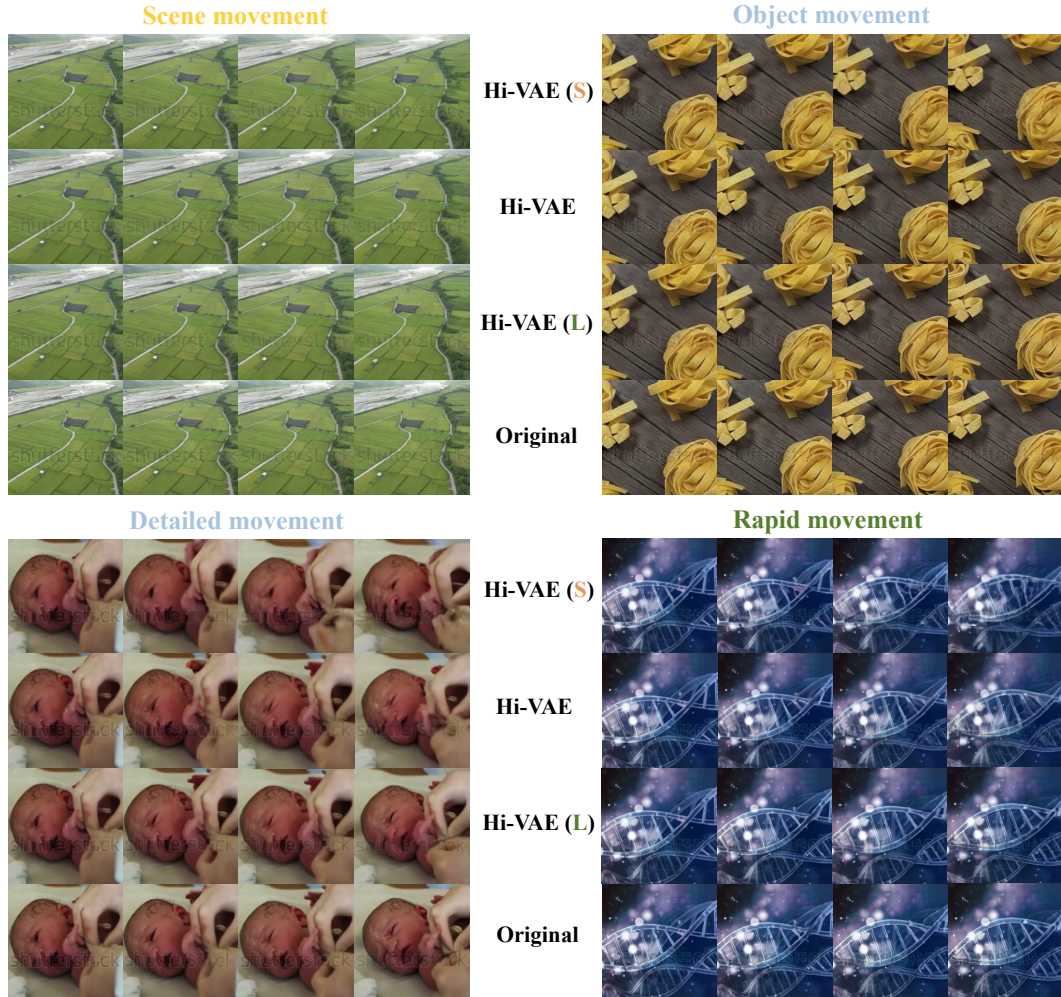


Figure 8: **Reconstruction Result** under different configurations.

movement, and rapid dynamic movement. Across all motion categories, Hi-VAE variants consistently maintain strong semantic fidelity and temporal consistency. Even Hi-VAE (S) with a compression rate of 0.07% achieves satisfactory reconstruction results. However, increased compression ratios introduce artifacts in fine details (e.g., eyes and hands of children). Preserving high-frequency details under extreme compression remains an important direction for future work.

C Additional Information on Experimental Settings

C.1 Definition of Compression Rate

Unlike the typical approach of representing the compression ratio using downsampling factors for height, width, and number of frames, we define it as the ratio between the dimensionality of the latent space utilized in the downstream model and the dimensionality of the input video. For instance, consider a video with a resolution of 256×256 pixels and 16 frames. If its downsampling factors for height, width, and number of frames are (8, 8, 4) respectively, and the channel dimension is 16, according to our definition, its compression ratio is 2.08%.

C.2 Standardized DiT for Resource Consumption Evaluation

Our Hi-VAE model constructs highly compressed motion latents, significantly reducing the resource requirements of downstream generative models. To validate this advantage, in Sec. 4.3, we compare

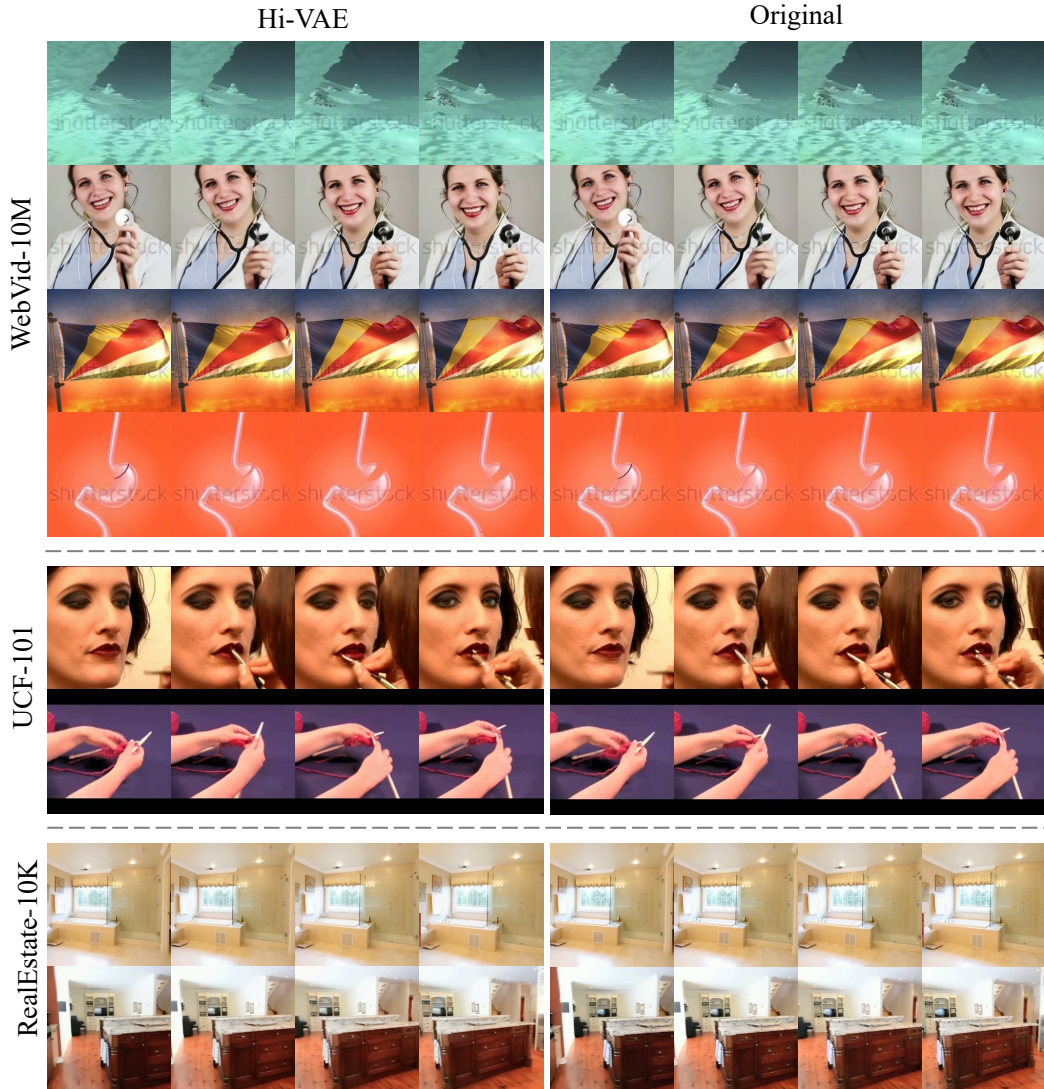


Figure 9: **Reconstruction Result** on diverse datasets.

the performance of generative models built upon Hi-VAE and baseline methods. To ensure fairness, all experiments adopt the DiT [29] architecture with the following configuration: an 8-layer network, 8 attention heads, a 512-dimensional hidden layer, and a 2048-dimensional feed-forward network. The computational complexity (FLOPs) is calculated based on a single sample (batch size=1). For the memory consumption test, the Adam [9] optimizer is employed, and the peak GPU memory usage during training is recorded.

D Additional Reconstruction Results

To thoroughly verify the generalizability of our approach, we supplemented the reconstruction results on diverse datasets. As depicted in Figure 9, these results convincingly demonstrate the superior reconstruction capabilities of our approach.